Supporting Information

Regulating Sequence Distribution of Polyethers *via ab initio* Kinetics Control in Anionic Copolymerization

Zhichao Wu[a†], Pei Liu[b†], Yu Liu[a], Wei Wei[a], Xinlin Zhang[a], Ping Wang[d], Zhenli Xu[bc] and Huiming Xiong[ac*]

[a]Department of Polymer Science, School of Chemistry and Chemical Engineering; [b]School of Mathematical Sciences and Institute of Natural Sciences; [c]Center for Soft Matter and Interdisciplinary Sciences, Shanghai Jiao Tong University, Shanghai 200240, P. R. China; [d]Dow Chemical (China) Investment Co., Ltd, Shanghai 201203, P. R. China.

* Corresponding author: hmxiong@sjtu.edu.cn

1. Experimental Procedures

1.1 Synthesis of monomer C

Synthesis of 1-(6-alkenyl-1-alkoxy)-4-(4-amyl-cyclohexyl) benzene

1,4-Dibromobutane (39.2 mL, 0.324 mol), 4-(4-pentylcyclohexyl)phenol(7.35 g, 29 mmol), KOH(1.6 g, 29 mmol), K_2CO_3 (4 g, 29 mmol), CH_3OH (50 mL), acetone (150 mL) were added into a two-necked flask with a fitted stirring bar. The reaction mixture was stirred at 65 °C for 24 h. The solution was filtered and then concentrated under reduced pressure. The mixture was recrystallized with 60 mL ethanol to yield white crystalline powder (8.9 g, 85%). ^{1}H NMR spectrum of 1-(6-alkenyl-1-alkoxy) -4-(4-amyl cyclohexyl) benzene was shown in Fig. S2.

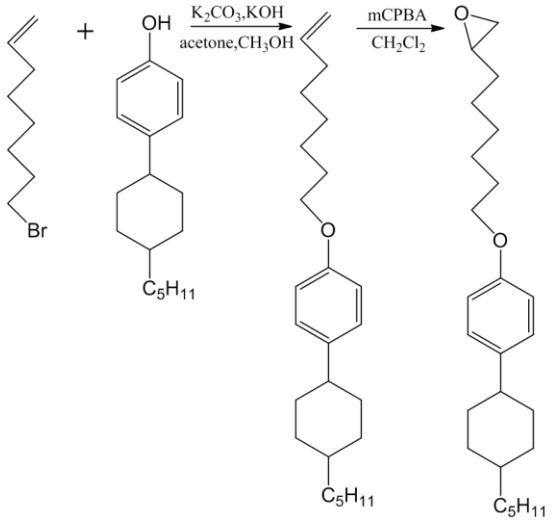

Figure S1. The schematics of the synthesis route of monomer C.

Synthesis of 2-(5-(4-(4-pentylcyclohexyl)phenoxy)pentyl)oxirane (C)

Chloroperoxybenzoic acid (CPBA, 4.65 g, 17.5 mmol) was dissolved in 50 mL dichloromethane and added into a two-necked flask with a fitted stirring bar. 1-(6-alkenyl-1-alkoxy)-4-(4-amyl-cyclohexyl) benzene (5 g, 13.4 mmol) was dissolved in 50 mL dichloromethane, and added drop-wise. The reaction mixture was stirred at RT for 24 h. The solution was then filtered and poured

into an 15% sodium sulphite aqueous solution. The organic layer was separated and then poured into an 15% potassium carbonate aqueous solution. The organic phase was collected in a flask. Anhydrous magnesium sulfate powder was added to dry the solution for 12 h. The solution was then filtered and concentrated via a rotary evaporator. The mixture was further purified by chromatography (SiO_2, ethyl acetate/hexane (1:60)) to yield white crystalline powder (3.7 g, 77%). ^{1}H NMR spectrum of 2-(5-(4-(4-pentylcyclohexyl)phenoxy)pentyl)oxirane (C) was shown in Fig. S3.

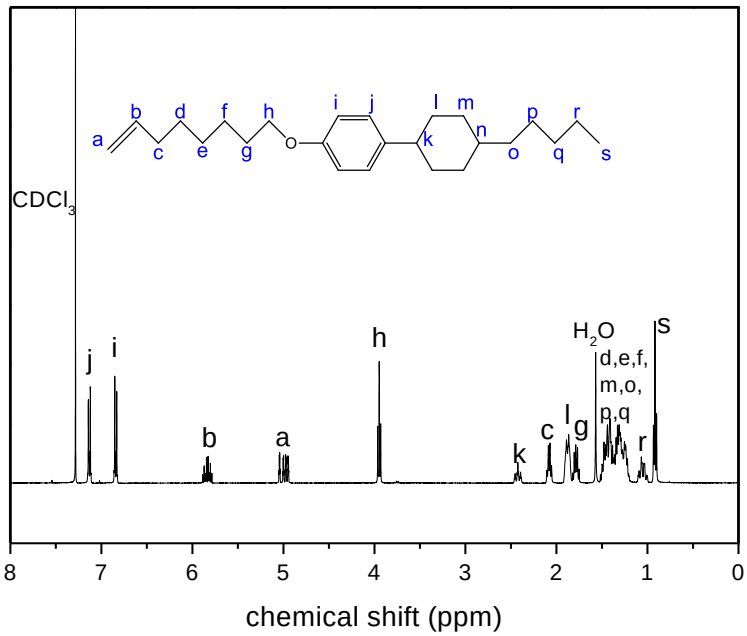

Figure S2. ^{1}H NMR spectra of 1-(6-alkenyl-1-alkoxy)-4-(4-amyl cyclohexyl)benzene.

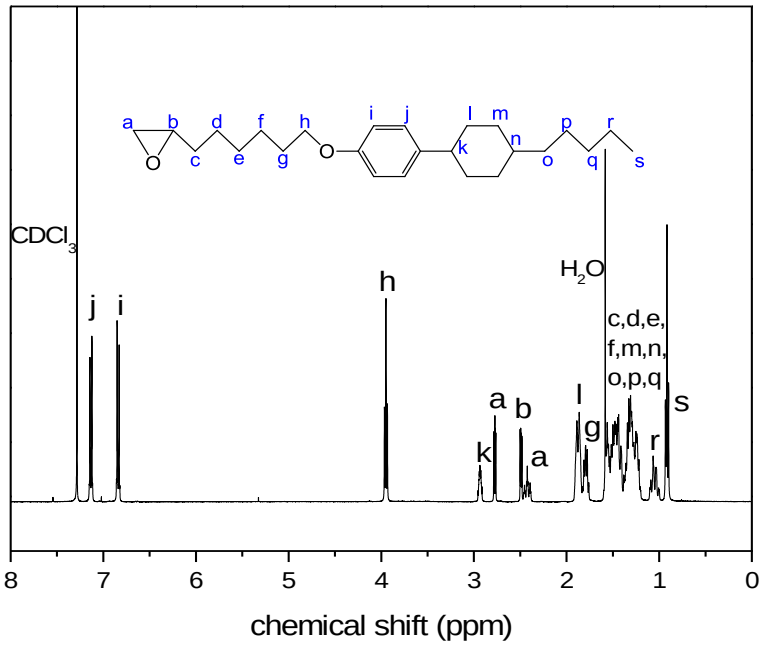

Figure S3. ^{1}H NMR spectra of 2-(5-(4-(4-pentylcyclohexyl)phenoxy)pentyl)oxirane.

1.2 Copolymerization and characterization

The monomers for copolymerization are 1,2-butylene oxide (monomer B), 2-(5-(4-(4-pentylcyclohexyl)phenoxy)pentyl)oxirane (monomer C), 2-((4-(4-(4-pentylcyclohexyl)phenoxy)butoxy)methyl)oxirane (monomer E) and 1-(4-methoxyphenyl)-2-(4- ((6-(oxiran-2-ylmethoxy)hexyl)oxy)phenyl)diazene (monomer A). Monomer B was obtained from commercial sources. Monomer E and A was synthesized in our laboratory following the similar procedure as previously described.[1,2] Monomer C was synthesized as described above. The anionic copolymerization procedure has already described in the main text.

Real-time ^{1}H-NMR spectra

A typical series of ^{1}H-NMR spectra for the copolymerizations of different monomer groups are shown in Fig. S4~S11. The chemical shifts of protons in oxirane groups of different monomers were well-resolved and can be identified to determine the consumption of the monomers during the copolymerization, as illustrated in the zoom-in spectra. The intensities of these monomers decayed with time of copolymerization. By following the integrals of the characteristic resonances of these monomers, the concentration profiles of the monomers *versus* the reaction time can be obtained, which are further utilized to calculate the kinetic parameters of the copolymerizations.

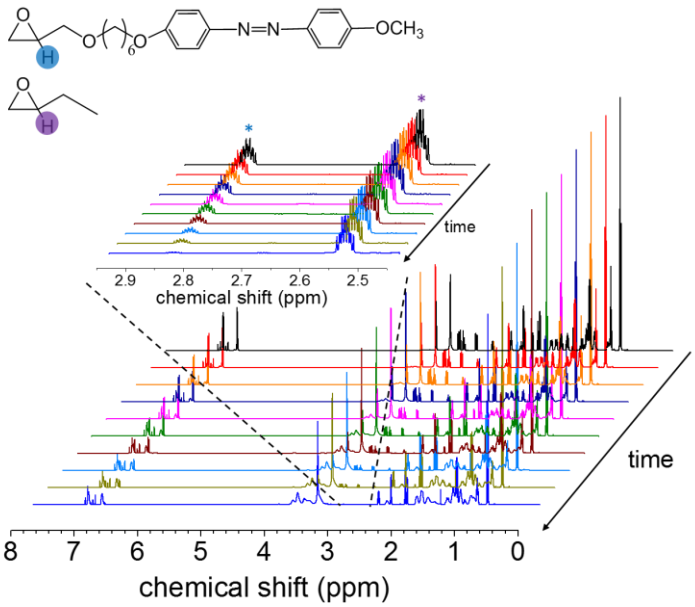

Figure S4. Real-time ^{1}H-NMR spectra overlay of copolymerization of monomer E and B (the bottom); the zoom-in spectral region (the top) used to determine the consumption of each monomer.

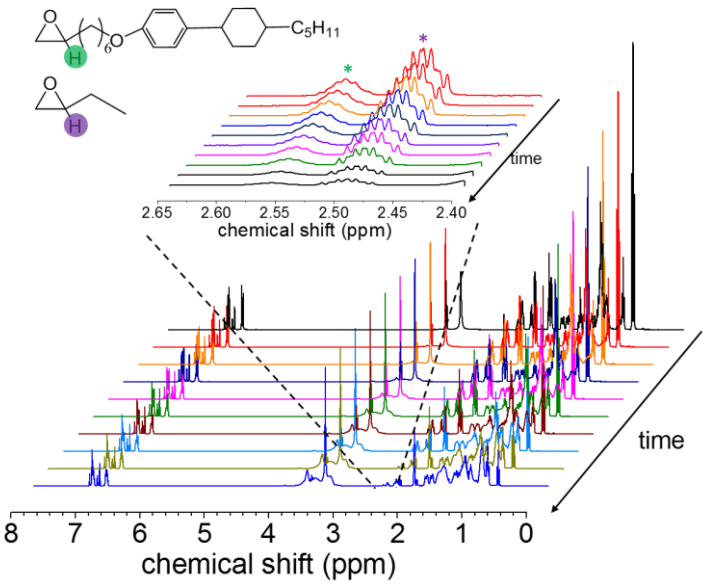

Figure S5. Real-time ^{1}H-NMR spectra overlay of copolymerization of monomer C and B (the bottom); the zoom-in spectral region (the top) used to determine the consumption of each monomer.

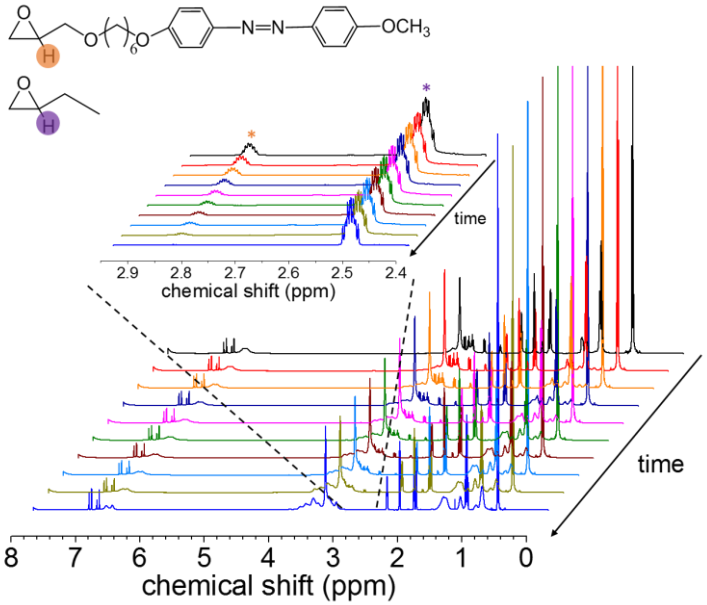

Figure S6. Real-time ^{1}H-NMR spectra overlay of copolymerization of monomer A and B (the bottom); the zoom-in spectral region (the top) used to determine the consumption of each monomer.

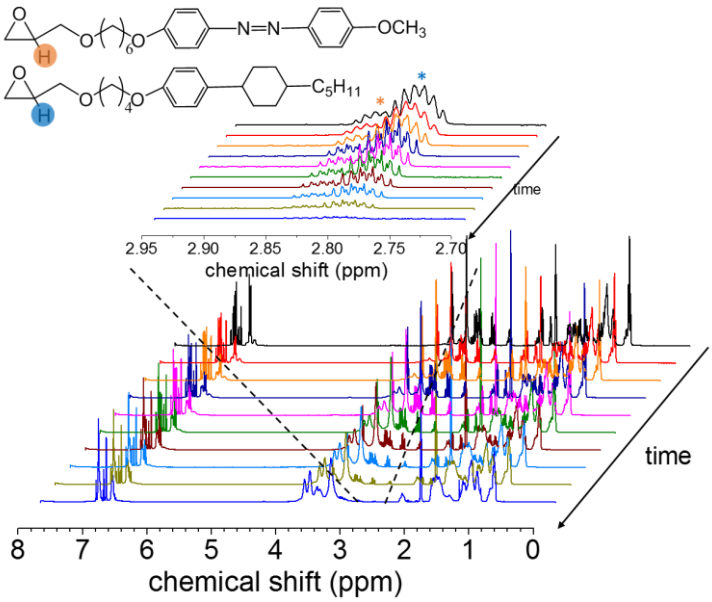

Figure S7. Real-time ^{1}H-NMR spectra overlay of copolymerization of monomer A and E at 1:3 feed ratio (the bottom); the zoom-in spectral region (the top) used to determine the consumption of each monomer.

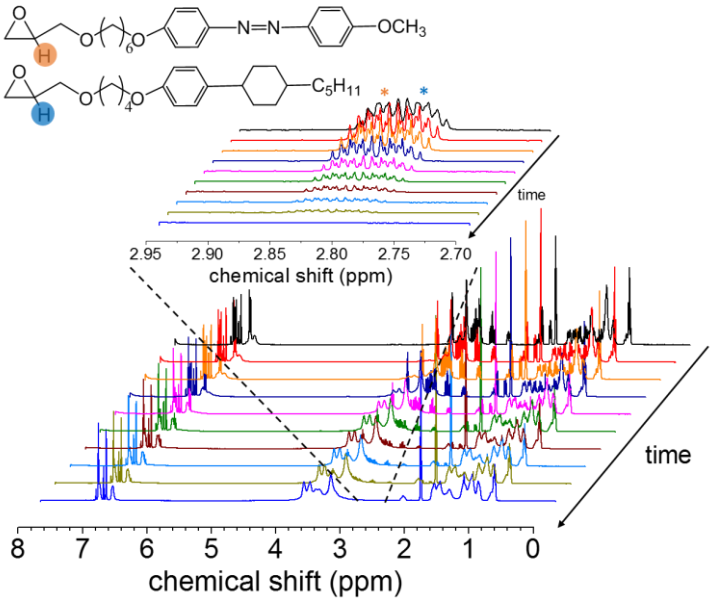

Figure S8. Real-time ^{1}H-NMR spectra overlay of copolymerization of monomer A and E at 1:1 feed ratio (the bottom); the zoom-in spectral region (the top) used to determine the consumption of each monomer.

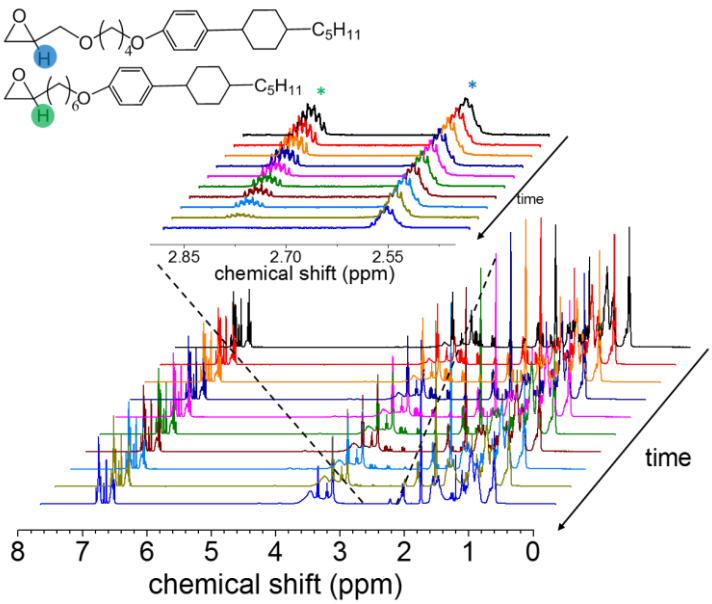

Figure S9. Real-time ^{1}H-NMR spectra overlay of copolymerization of monomer E and C (the bottom); the zoom-in spectral region (the top) used to determine the consumption of each monomer.

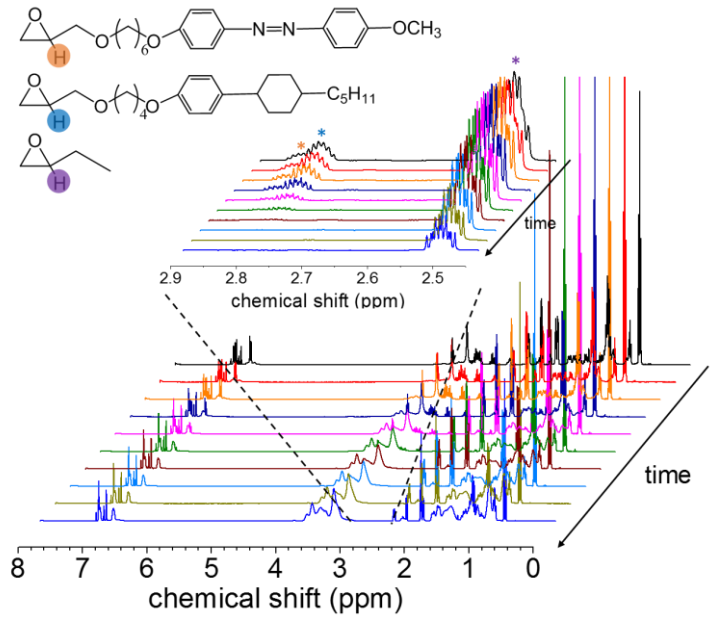

Figure S10. Real-time ^{1}H-NMR spectra overlay of copolymerization of monomer A, E and B (the bottom); the zoom-in spectral region (the top) used to determine the consumption of each monomer.

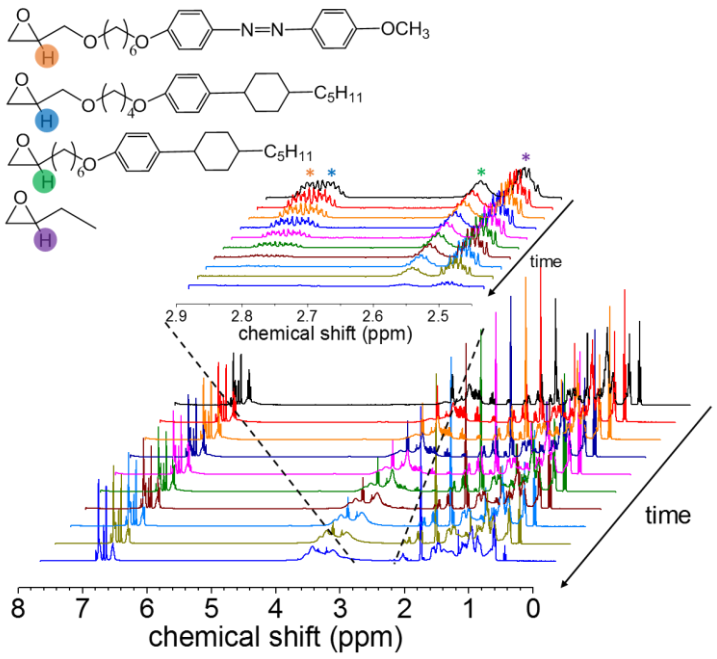

Figure S11. Real-time ^{1}H-NMR spectra overlay of copolymerization of monomer A, E, C and B (the bottom); the zoom-in spectral region (the top) used to determine the consumption of each monomer.

2. Fitting Results and Discussion.

2.1 Fitting program

Mathematical model

The copolymerization supposedly performs in a binary system of monomers M_1 and M_2, and the time evolutions of monomer concentrations, $[M_1]_t$ and $[M_2]_t$, are experimentally obtained, where $t = 1, 2, \dots, n_s$ stands for each time step. The total concentration of active species $[M_1^* + M_2^*]$ is known and conserved during the copolymerization. With certain initial values of $[M_1]_{t=0}$, $[M_2]_{t=0}$, $[M_1^*]_{t=0}$ and $[M_2^*]_{t=0}$, the time evolutions of monomer concentrations can be described through the master equations (1),

$$\begin{cases} \frac{d}{dt}[M_1] = -k_{11}[M_1^*][M_1] - k_{21}[M_2^*][M_1], \\ \frac{d}{dt}[M_2] = -k_{12}[M_1^*][M_2] - k_{22}[M_2^*][M_2], \\ \frac{d}{dt}[M_1^*] = -k_{12}[M_1^*][M_2] + k_{21}[M_2^*][M_1], \\ \frac{d}{dt}[M_2^*] = k_{12}[M_1^*][M_2] - k_{21}[M_2^*][M_1], \end{cases} \quad (1)$$

where the reaction coefficients k_{11}, k_{12}, k_{21} and k_{22} are unknown parameters to be determined.

We develop a numerical method to find the best set of parameters such that the numerically computed monomer concentrations *versus* time fit well with the experimental data.[3] The reaction coefficients k_{11}, k_{12}, k_{21} and k_{22}, together with the initial values of $[M_1]_{t=0}$ and $[M_2]_{t=0}$, are solved through the fitting program, while the initial values $[M_1^*]_{t=0}$ and $[M_2^*]_{t=0}$ are given by the steady state assumption at $t = 0$,

$$\begin{cases} [M_1^*]_{t=0} = \frac{k_{12}[M_1]_{t=0}}{k_{21}[M_1]_{t=0} + k_{12}[M_2]_{t=0}}[M_1^* + M_2^*]_{t=0}, \\ [M_2^*]_{t=0} = \frac{k_{21}[M_2]_{t=0}}{k_{21}[M_1]_{t=0} + k_{12}[M_2]_{t=0}}[M_1^* + M_2^*]_{t=0}. \end{cases} \quad (2)$$

The master equations are numerically solved through 4th order Runge-Kutta scheme,[4] and the numerical concentrations at time t are denoted by $\widetilde{M_{1,t}}$ and $\widetilde{M_{2,t}}$. The objective function is defined as

$$\varepsilon = \sqrt{\frac{1}{n_s}\sum_{t=1}^{n_s}[(\widetilde{M_{1,t}} - M_{1,t})^2 + (\widetilde{M_{2,t}} - M_{2,t})^2]} + \mu(k_{11}k_{22} - k_{12}k_{21})^2, \qquad (3)$$

which provides the measure of how good the fit is, that is, how close to $M_{1,t}$ and $M_{2,t}$ the data sets $\widetilde{M_{1,t}}$ and $\widetilde{M_{2,t}}$ will be. The first term in Eq. (3) is the mean square root error between the numerical results and the experimental data which described as error in Table S4. The second term is the penalty term, which can be used to constrain the copolymerization approaching to the ideal behavior. If $\mu \to \infty$, it is equivalent to a constraint $k_{11}k_{22} = k_{12}k_{21}$. That means the product of the reactivity ratios is $r_1 \times r_2 = 1$ and the copolymerization is ideal, which is the usual case for the anionic copolymerization. If $\mu = 0$, there is no extra knowledge about the reactivity ratios. In our fittings, the penalty is often used to a certain degree.

Global optimization strategy

Whether the objective function ε is convex or not as a function of the reaction coefficients k_{11}, k_{12}, k_{21}, k_{22} and the initial values $[M_1^*]_{t=0}$, $[M_2^*]_{t=0}$ is not proven. Usually, convex optimization methods only guarantee a local convergence for non-convex problems so that a good initial guess is often needed. To overcome this difficulty, we first employ the simulated annealing strategy, which is a metaheuristic to approximate global optimization in a large search space.[5] To find the best set of parameters, we iteratively choose a new set from the previous one. By comparing their values of the corresponding objective functions, we accept/reject this new one with a certain probability so that we can generate a distribution $\sim e^{-\varepsilon/T}$, where T is the artificial temperature. The globally convergence is guaranteed if the annealing process is sufficiently slow. When T is small enough, only those states around minimum ε can be achieved. Instead of setting $T = 0$ in the final iterations, at a threshold small value of temperature, we employ the gradient descent method with backtracking line search, using the parameters given by the simulated annealing as good initial guesses. Our method avoids the possible failure of direct using gradient descent methods or Newton's methods in finding the correct reaction coefficients. It is found generally applicable in fitting our experimental data.

Test examples

To validate our numerical methods, we first have checked with some test examples with exactly given chemical reaction coefficients and initial concentrations of monomers and active species. The time evolutions of monomer concentrations are computed numerically with very small time step, so that they can be viewed as the exact solution of the master equation (1). In order to mimic the experimental error, we add white noises of amplitude δ to $[M_1]_t$ and $[M_2]_t$. When applying our program to the data sets $[M_1]_t$ and $[M_2]_t$, the fitting values of the chemical reaction coefficients should be close to the exactly given parameters if δ is small. In Table S1 and Table S2, we show the fitting results for the test examples. The exact solution is chosen to be the parameters computed from the A-co-B sample in our experiments as an example: $k_{11} = 0.0301$ g mmol^{-1} min^{-1}, $k_{21} = 0.00364$ g mmol^{-1} min^{-1}, $k_{12} = 0.00503$ g mmol^{-1} min^{-1}, $k_{22}=(k_{21}\times k_{12})/k_{11}$ =0.000608 g mmol^{-1} min^{-1}, $[M_1]_{t=0} = 1.343$ mmol g^{-1}, $[M_2]_{t=0} = 6.714$ mmol g^{-1}, and $[M_1^* + M_2^*]_{t=0} = 0.166$ mmol g^{-1}.

Table S1. Fitting results computed with different white noise amplitudes and with penalty.

μ	10^{10}						
δ（mmol g^{-1}）	0.01	0.02	0.03	0.04	0.05	0.06	0.1
k_{11}（g mmol^{-1} min^{-1}）	0.030052	0.030192	0.030050	0.030065	0.030217	0.030074	0.029642
k_{21}（g mmol^{-1} min^{-1}）	0.003634	0.003636	0.003635	0.003611	0.003627	0.003706	0.003685
k_{12}（g mmol^{-1} min^{-1}）	0.005027	0.005056	0.005017	0.005068	0.005077	0.004978	0.004839
k_{22}（g mmol^{-1} min^{-1}）	0.000608	0.000608	0.000607	0.000607	0.000609	0.000613	0.000601
$[M_1]_{t=0}$（mmol g^{-1}）	1.343015	1.342995	1.343011	1.343001	1.342997	1.342994	1.343012
$[M_2]_{t=0}$（mmol g^{-1}）	6.713999	6.714004	6.713996	6.714003	6.714004	6.713995	6.713963

Table S2. Fitting results computed with different white noise amplitudes and without penalty.

μ	0						
δ（mmol g^{-1}）	0.01	0.02	0.03	0.04	0.05	0.06	0.1
k_{11}（g mmol^{-1} min^{-1}）	0.030051	0.029920	0.030092	0.030217	0.030018	0.029964	0.030186
k_{21}（g mmol^{-1} min^{-1}）	0.003639	0.003686	0.003663	0.003614	0.003640	0.003739	0.003826
k_{12}（g mmol^{-1} min^{-1}）	0.005051	0.005224	0.005155	0.005086	0.005092	0.005109	0.005616
k_{22}（g mmol^{-1} min^{-1}）	0.000607	0.000602	0.000603	0.000607	0.000608	0.000609	0.000582
$[M_1]_{t=0}$（mmol g^{-1}）	1.343002	1.342997	1.343021	1.342997	1.342001	1.343002	1.342989
$[M_2]_{t=0}$（mmol g^{-1}）	6.714002	6.713996	6.714006	6.714003	6.714004	6.714001	6.713983

These fitting results clearly show that the fitting program works well and can find the proper reaction coefficients. The ideal copolymerization condition $r_1r_2 = (k_{11}k_{22})/(k_{12}k_{21}) = 1$ or the penalty μ is not essential, as demonstrated in Fig. S12. However, it could help fitting sometimes since it provides extra constraints, especially when the amplitude of white noise is large. We use the penalty in our fitting.

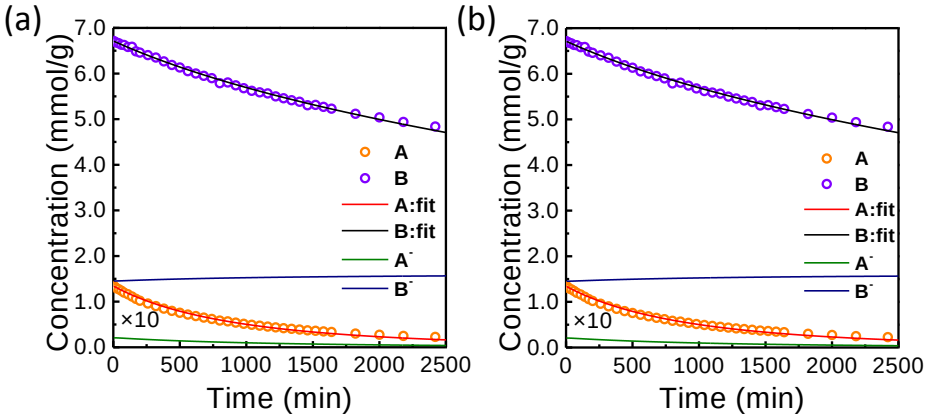

Figure S12. Fitting results for $\delta = 0.05$. (a) $\mu = 10^{10}$; (b) $\mu = 0$; $[A^*]_0$ and $[B^*]_0$ are chosen initially as 0.021 mmol g^{-1} and 0.145 mmol g^{-1}.

2.2 Fitting results

The fittings are run by the program written by C++ language. And the program also allows two or more data groups calculated in parallel which we have used in fitting the A-co-E (1:1) group and A-co-E (1:3) group. In the end, the four reaction rate constants and the concentration changes of the active reactants are obtained, consequently, the reactivity ratios of the monomers can be derived.

Each data group had been calculated for several times by the same parameter setting to check the convergence of the results. We chose the fitting result which has minimum error to be the arithmetic solution. The reaction rate constants calculated by the fitting program of all the copolymerization groups are summarized in Table S3. All the fitting results are showed in Fig. S13. The derived concentrations of anionic species have been multiplied by a suitable number to make them visible on the same scale.

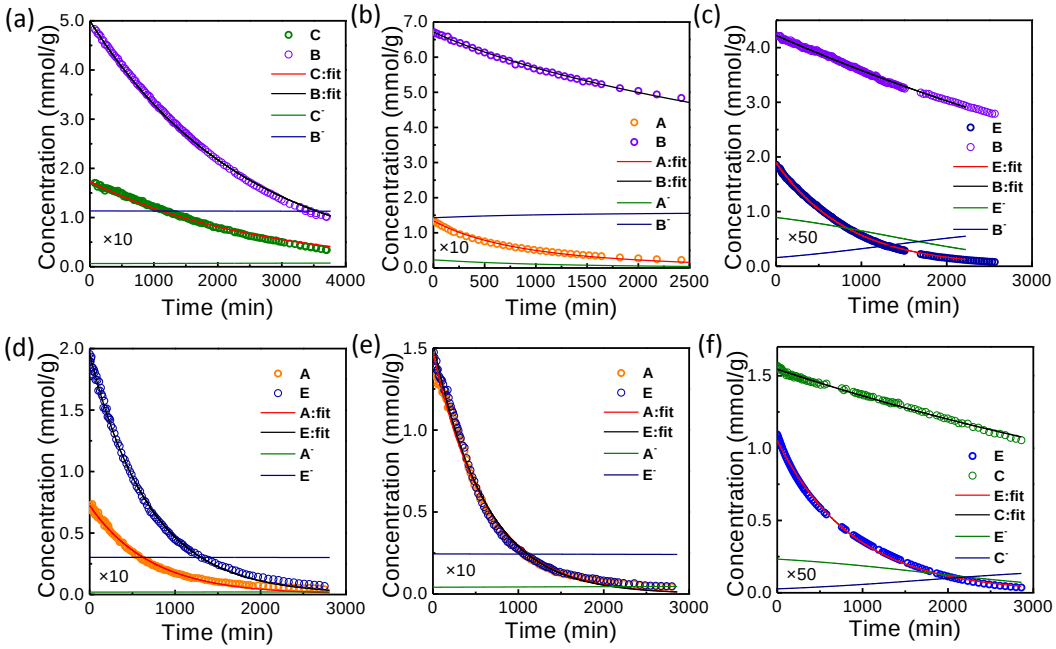

Figure S13. Time-dependent concentrations of monomers obtained by real-time NMR experiments and their fits with the kinetic model. (a) C-co-B, (b) A-co-B, (c) E-co-B, (d) A-co-E (1:3), (e) A-co-E (1:1), (f) E-co-C.

Table S3. The reactivity ratio of each copolymer group obtained by fitting.

Copolymer sample	k_{11} (g mmol^{-1} min^{-1})	k_{12} (g mmol^{-1} min^{-1})	k_{21} (g mmol^{-1} min^{-1})	k_{22} (g mmol^{-1} min^{-1})	r_1	r_2	Error* (mmol g^{-1})
C-co-B	0.0138	0.0152	0.00252	0.00277	0.91	1.1	0.0593
A-co-B	0.0301	0.00503	0.00364	0.000608	6.0	0.17	0.0408
E-co-B	0.0510	0.00698	0.0874	0.0119	7.3	0.14	0.0304
A-co-E	0.192	0.200	0.0338	0.0345	0.96	1.02	0.0592
E-co-C	0.206	0.0233	0.292	0.0342	8.8	0.12	0.0198

* The mean square root error between the numerical results and the experimental data as described in Eq. (3).

Note:

The code is available upon request.

References:

1. Y. Liu, W. Wei and H. M. Xiong, *Polymer,* 2013, **54**, 6572.
2. Y. Liu, W. Wei and H. M. Xiong, *Polym. Chem.,* 2015, **6**, 583.
3. Z. C. Wu, Y. Liu, W. Wei, F. S. Chen, G. X. Qiu and H. M. Xiong, *Chinese J. Polym. Sci.*, 2016, **34**, 431.
4. J. C. Butcher, *Numerical Methods for Ordinary Differential Equations, 2nd Edition*; John Wiley & Sons: New York, 2008.
5. C. T. Kelley, *Iterative Methods for Optimization*; SIAM Philadelphia, 1999.